

MASS-TRANSFER COEFFICIENTS IN PACKED BEDS AT VERY LOW REYNOLDS NUMBERS

PETER S. FEDKIW* and JOHN NEWMAN

Materials and Molecular Research Division, Lawrence Berkeley Laboratory and Department of Chemical Engineering, University of California, Berkeley, CA 94720, U.S.A.

(Received 12 May 1981 and in revised form 16 November 1981)

Abstract—Accurate, transport-controlled, mass transfer coefficients for packed beds have been measured by an electrochemical technique at low Reynolds numbers ($0.00271 < v/av < 0.198$). At low Péclet numbers, the data show a strong dependence upon the bed length, but this dependence diminishes at the higher flow rates. The results are correlated by a dual-sized, straight-pore model for the bed's pore volume.

The bed behaves as though 1.46% of the pore volume were in pores whose diameter is 56% greater than the diameter of the remaining pores. The larger pores result in a flow maldistribution and significantly reduce mass transfer at the lower Péclet numbers.

NOMENCLATURE

A ,	dimensionless amplitude of sinusoidal, periodically constricted tube (PCT);
a_i ,	specific interfacial area of tube size i matrix [cm^{-1}];
a ,	$= a_1 + a_2$, specific interfacial area of entire bed [cm^{-1}];
B ,	$= (1 + \sqrt{1 + 4D'})/2$;
c_F ,	reactant feed concentration [mol/cm^3];
$c_{L,i}$,	reactant concentration exiting from tube size i matrix [mol/cm^3];
c_L ,	reactant concentration exiting from bed [mol/cm^3];
d_p ,	diameter of packing particle [cm];
D' ,	$= \epsilon a k_f E/v^2$;
\mathcal{D}_0 ,	free stream reactant diffusivity [cm^2/s];
E ,	dispersion coefficient [cm^2/s];
h ,	defined by equation (20);
k_f ,	film mass transfer coefficient [cm/s];
k_m ,	effective mass transfer coefficient for bed [cm/s];
L ,	bed length [cm];
n ,	empirical constant;
Pe_i ,	$= v_i/a\mathcal{D}_0$, Péclet number for tube size i matrix;
Pe_B ,	$= v/a\mathcal{D}_0$, Péclet number for bed;
q_i ,	flowrate in tube size i [cm^3/s];
Q_i ,	collective flowrate in tube size i matrix [cm^3/s];
r_i ,	radius of tube size i [cm];
r_A ,	dimensionless radius of PCT;
Re_B ,	$= v/av$, Reynolds number;
Sh_i ,	$= \epsilon k_{m,i}/a_i\mathcal{D}_0$, Sherwood number for tube size i matrix;
Sh_B ,	$= \epsilon k_m/a\mathcal{D}_0$, Sherwood number for bed;
v_i ,	superficial velocity in tube size i matrix [cm/s];

v ,

z ,

$v_1 + v_2$, superficial velocity in bed [cm/s];

streamwise coordinate [cm].

Greek symbols

α ,	$= ak_f/v$ [cm^{-1}];
γ ,	$= Q_2/Q_1$;
ε_i ,	porosity of tube size i matrix;
ε ,	$= \varepsilon_1 + \varepsilon_2$, bed porosity;
δ ,	$= r_2/r_1$;
ν ,	kinematic viscosity [cm^2/s];
σ ,	fitting coefficient in equation (6).

INTRODUCTION

MANY REFERENCES in the chemical engineering literature report mass transfer coefficients in packed beds. Understandably, very few of these works have been directed at studying mass transfer rates at very low Reynolds numbers ($\ll 1$). There is a need, however, to characterize the fluid-to-particle transport rate at very low Reynolds numbers, for example, the flowrate in flow-through porous electrodes must often be in a region of very low ($\ll 1$) Reynolds number in order to minimize the detrimental ohmic potential drop [1].

This paper reports an experimental study of transport-controlled mass transfer coefficients at low Reynolds numbers (< 1) in a packed-bed reactor. The results are correlated by a model which incorporates a flow-maldistribution (channelling) effect. The work presented in this paper represents the final report in an effort to characterize on a more fundamental basis the mass transfer rate in packed-bed reactors [2-5].

MASS TRANSFER COEFFICIENT

There are two mass transfer coefficients that can be used to characterize the reaction rate in packed beds. The so-called film coefficient k_f represents the proportionality constant between the local reaction rate and the local concentration driving force. The film coefficient appears on the right side of the conservation

* Present address: Department of Chemical Engineering, North Carolina State University, Raleigh, NC 27650, U.S.A.

equation for the reactive species as written in equation (1) for a mass transfer controlled reaction:

$$E \frac{d^2c}{dz^2} - v \frac{dc}{dz} = ak_f c. \quad (1)$$

The film mass transfer coefficient is a measure of the local reaction rate in the bed. It is a quantity that is not very convenient to measure. The concentration of the reactant far upstream and far downstream of a reactor is more readily accessible to experimental determination. These measurements are correlated by the effective mass transfer coefficient k_m . In the mass transfer controlled reactor under discussion, the definition of k_m is

$$k_m = \frac{v}{aL} \ln (c_F/c_L). \quad (2)$$

These two mass transfer coefficients are related as has been pointed out by [1];

$$k_m = \frac{k_f}{B} + \frac{v}{aL} \times \ln \left\{ \frac{B + \frac{D'}{B^2}(1-B) \exp \left[-\alpha L \left(\frac{1}{B} + \frac{B}{D'} \right) \right]}{1 + D'/B^2} \right\}. \quad (3)$$

If so desired, the experimental k_m measurements can be corrected by equation (3) to give k_f . An expression for the dispersion coefficient is, however, required. The distinction between the two coefficients is unimportant at high Reynolds numbers. At low Reynolds numbers, the two coefficients show different dependencies on the flowrate, as has been discussed previously [3].

Shown in Fig. 1 are k_m data (expressed as a Sherwood number) found in the literature as a function of the Péclet number. Each of these data points was collected in a mass transfer controlled bed with the Reynolds number (v/av) less than one. Both gas and liquid phase data are included. The Péclet number is the most appropriate grouping to characterize the mass transfer rates at low Reynolds numbers (creeping flow).

Note that $(1/a)$ has been chosen as the characteristic length in lieu of the packing particle diameter. For a bed of uniformly sized spheres, these two length scales are related by $ad_p = 6(1 - \varepsilon)$.

The lines sketched on this figure are drawn only to indicate the asymptotic trends of k_m with the Péclet number (v/aD_0). Clearly, there are different trends. In the lower Péclet number range, k_m becomes linearly proportional to the velocity v , whereas in the higher Péclet number range k_m becomes proportional to $v^{1/3}$. This second line is a plot of Wilson and Geankoplis' correlation [12]:

$$\frac{k_m d_p}{D_0} = \frac{1.09}{\varepsilon} \left(\frac{vd_p}{D_0} \right)^{1/3}. \quad (4)$$

Most of the data reported are taken in relatively

shallow beds. The aL product ranges from 3 (one particle layer) to 29.

There is considerable scatter in the data shown. The differences between different authors is certainly evident. Also noteworthy is the large degree of scatter in the data confined to one author, particularly at the lower Péclet numbers.

Theoretical calculations [14] have predicted in creeping flow that the mass transfer coefficient should be dependent upon the length of the reactor. The validity of those calculations cannot be ascertained with the available data.

MASS TRANSFER COEFFICIENT MEASUREMENTS

The limiting-current procedure was used to measure the transport-limited mass transfer coefficients [6]. A schematic of the apparatus is shown in Fig. 2, and a summary of the procedure given below. The reader interested in more details should consult [15].

Summary of procedure

A randomly packed bed of uniform-size, 3.175 mm (1/8" dia.), copper plated, stainless steel bearings was used as the cathode in a glass, thermostatted, electrochemical, flow-through reactor 76.2 mm in diameter. Copper was plated on the surface of these particles from an acidified (1 M H_2SO_4) copper sulfate solution. Copper deposition was chosen as the test reaction because atomic absorption could be used to measure accurately the ion concentration at the lower concentrations used (0.1 p.p.m.) with an uncertainty of $\pm 1\%$. The evolution of O_2 in a separate compartment was the anode reaction. Sufficient cathodic polarization was applied to the bed to ensure that the deposition reaction was controlled by the transport of the Cu^{2+} ions to the particle surface. This transport controlled reaction manifests itself as a limiting-current plateau on a plot of current vs applied potential. The overall reaction rate for the copper deposition can be measured by two independent techniques: (i) the inlet and outlet Cu^{2+} concentration is determined and (ii) the cell current is measured. The latter is, according to Faraday's Law (assuming negligible side reactions) proportional to the amount of copper consumed. These two independent measurements permit a cross verification of the mass transfer coefficients calculated from the data. Only those data that gave mass transfer coefficients which deviate $\pm 5\%$ from the average are reported. All other data were rejected. The experimental variables which were manipulated were the flowrate of the feed solution, the Schmidt number of the feed (by addition of glycerol), and the packing depth. The Reynolds number (v/av) varied from 0.198 to 0.00271; two values of Schmidt number were studied, 1900 and 8880, and the bed depth could be characterized by $aL = 30$ and 100.

A total of 59 runs yielded k_m data which meet the specification given above. The reduced data for these runs are presented in Table 1 and are compared with Appel and Newman's data for a shorter bed on Fig. 3.

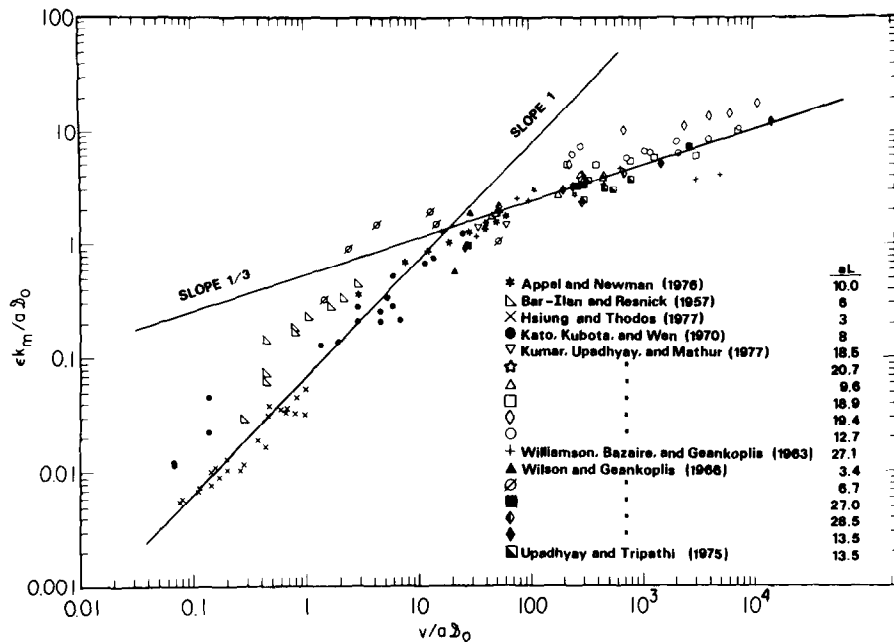


FIG. 1. Low Reynolds number mass transfer coefficients in packed beds.

A clear dependency of Sh_B on aL at the lower Péclet numbers is seen, and this dependency diminishes as the Péclet number increases.

MASS TRANSFER COEFFICIENT CORRELATION

In a series of earlier papers the authors have calculated predicted Sherwood numbers for a bed when the void space between the packing was envisioned as a sinusoidal PCT. The following limiting Sherwood numbers were calculated:

$Sh_B^{(1)}$ = low Péclet number, deep bed asymptotic Sherwood number,

$Sh_B^{(2)}$ = high Péclet number, deep bed asymptotic Sherwood number,

$Sh_B^{(3)}$ = high Péclet number, entrance region asymptotic Sherwood number,

$Sh_B^{(4)}$ = high Péclet number, mixing region Sherwood number.

An attempt was made to combine these asymptotic Sherwood numbers smoothly in some manner to cover the non-asymptotic regions and compare the predictions with the data in Fig. 3. Churchill and Usagi [16], expanding upon an idea suggested by Acrivos [17], have pointed out a manner to combine asymptotic formulae. Their procedure will be utilized here. As a first attempt, the model for the bed as an array of PCT leads one to write

$$\frac{1}{Sh_B} = \left[\left(\frac{1}{Sh_B^{(1)}} \right)^n + \left(\frac{1}{Sh_B^{(2)} + Sh_B^{(3)}} \right)^n \right]^{1/n}. \quad (5)$$

This is not a unique representation, but it is the simplest. The exponent n must be determined by a data-fitting procedure.

The usefulness of combining the asymptotic formulae as suggested in equation (5) can be found by testing it with Sørensen and Stewart's [14] calcu-

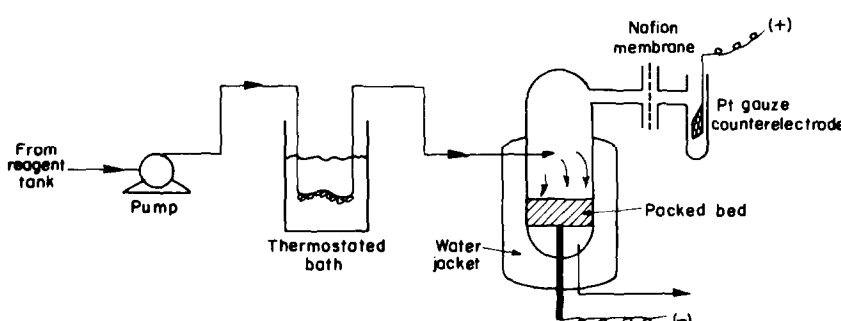


FIG. 2. Schematic of packed bed electrode cell.

Table 1. Calculated results

Run	ϵ	aL	$\frac{vd}{v}$	$\frac{v}{av}$	$\frac{v}{\bar{v}_0}$	$\frac{v}{a\bar{v}_0}$	$\frac{\epsilon k_m}{a\bar{v}_0}$
10	0.366	30.1	0.213	0.0560	1900	107	1.69
11	0.391	29.0	0.409	0.112	1900	213	2.42
12	0.382	30.4	0.211	0.0568	1910	108	1.71
15	0.372	100	0.213	0.0565	1910	108	1.54
18	0.385	30.4	0.413	0.112	1887	211	2.50
19	0.374	30.3	0.413	0.110	1887	207	2.18
20	0.385	100	0.413	0.112	1887	211	2.11
21	0.406	30.3	0.0880	0.0247	1887	46.5	1.34
22	0.390	100	0.0878	0.0240	1903	45.9	1.04
24	0.390	29.1	0.125	0.0341	1903	65.0	1.48
25	0.393	29.7	0.0477	0.0131	1910	25.1	0.828
27	0.385	100	0.0450	0.0122	1894	23.2	0.477
28	0.385	100	0.0664	0.0180	1894	34.0	0.642
30	0.394	29.7	0.0436	0.0120	1894	22.8	0.767
31	0.392	30.4	0.165	0.0453	1921	87.1	1.80
32	0.396	30.5	0.0249	6.83×10^{-3}	1906	13.1	0.615
33	0.396	30.5	9.82×10^{-3}	2.71×10^{-3}	1906	5.20	0.330
34	0.396	30.5	0.137	0.0377	1906	71.8	2.07
35	0.392	101	0.0290	7.96×10^{-3}	1906	15.2	0.450
36	0.392	101	0.0522	0.0143	1906	27.2	0.683
37	0.392	101	0.169	0.0463	1906	88.2	1.50
40	0.400	30.4	0.0695	0.0193	1910	36.8	1.08
41	0.393	99.9	0.124	0.0340	1910	64.9	1.41
42	0.393	99.9	0.0503	0.0138	1910	26.5	0.897
43	0.393	99.9	0.104	0.0286	1910	54.6	1.26
44	0.393	99.9	0.185	0.0508	1910	97.1	1.78
45	0.393	99.9	0.230	0.0631	1910	121	2.10
47	0.393	99.9	0.341	0.0937	1910	179	2.55
48	0.393	99.9	0.370	0.107	1910	204	2.75
51	0.373	30.3	0.489	0.130	1915	249	2.86
52	0.373	30.3	0.564	0.150	1915	288	3.07
53	0.373	30.3	0.673	0.179	1915	343	3.22
55	0.383	100	0.288	0.0779	1926	150	1.99
56	0.383	100	0.515	0.139	1926	267	2.57
57	0.383	100	0.418	0.113	1926	218	2.41
58	0.383	100	0.581	0.157	1926	302	2.87
59	0.383	100	0.773	0.198	1926	382	3.33
61	0.400	29.9	0.0580	0.0161	1919	30.9	1.14
62	0.400	29.9	0.0162	4.50×10^{-3}	1919	8.63	0.523
63	0.400	29.9	0.0788	0.0219	1919	41.9	1.56
64	0.400	29.9	0.0343	9.54×10^{-3}	1919	18.3	0.935
65	0.400	29.9	0.141	0.0393	1919	75.3	2.10
66	0.400	29.9	0.209	0.0581	1919	111	2.53
67	0.387	100	0.0345	9.37×10^{-3}	1919	18.0	0.484
68	0.387	100	0.0222	6.03×10^{-3}	1919	11.6	0.332
69	0.387	100	0.0684	0.0186	1919	35.8	0.770
70	0.387	100	0.0953	0.0259	1919	49.7	1.08
71	0.387	100	0.141	0.0384	1919	73.7	1.34
72	0.387	100	0.0817	0.0222	1919	42.5	0.983
74	0.388	30.0	0.0210	5.73×10^{-3}	8880	50.9	1.55
75	0.388	30.0	8.92×10^{-3}	2.43×10^{-3}	8880	21.5	0.949
76	0.388	30.0	0.0299	8.19×10^{-3}	8880	72.1	1.85
77	0.388	30.0	0.0397	0.0108	8880	96.1	2.02
78	0.388	30.0	0.0485	0.0132	8880	117	2.25
79	0.388	30.0	0.0610	0.0166	8880	148	2.47
80	0.388	30.0	0.0782	0.0213	8880	189	2.88
81	0.388	30.0	0.102	0.0279	8880	248	3.21
82	0.388	30.0	0.133	0.0363	8880	322	3.57
83	0.388	30.0	0.174	0.0474	8880	421	4.08

lations. These authors have solved the convective diffusion equation in creeping flow for an array of uniformly sized, simple cubic packed spheres. They presented numerical calculations for k_m as a function of bed depth and Péclet number. They also presented formulae for the $Sh_B^{(i)}$, $i = 1, 2, 3$. Figure 4 is a plot of the

calculated k_m compared with that given by combination of the asymptotes according to equation (5) with $n = 1$. Even in this worse case the deviation appears acceptable.

The value of n to fit the experimental data was determined by fitting the 68 data points shown in Fig. 3 to equation (5) by using a non-linear, least squares procedure. The value depended upon the tube parameters used. Both a sinusoidal PCT model with $r_A = 1/2$, $A/r_A = 1/3$ and a straight tube model ($A/r_A = 0$) were tested against the data.

The data clearly indicate that in the lower Péclet numbers (< 10) the Sherwood number depends upon the packing depth. However, as the Péclet number increases, this length dependence diminishes. For Péclet numbers greater than 100, there is no significant distinction between the Sherwood number in a bed of $aL = 10$ vs $aL = 100$. At this Péclet number, the Reynolds number was approx. $100/2000 = 0.05$. Equation (5) could never reproduce this trend. It shows the strongest length dependence as the Péclet number increases due to the $Sh_B^{(3)}$ which is the only length-dependent term in equation (5).

In the high Péclet number region, the model calculations involved the assumption that the boundary layer formed along the particle surface retained its identity throughout the depth of the bed. It was anticipated that this would be true only in the creeping flow regime because any inertially caused mixing effects at higher Reynolds numbers would destroy the boundary layer. The higher Péclet number data suggest that the boundary layers do lose their identity. One can speculate as to the cause of this phenomenon at such low Reynolds numbers. Perhaps the lateral mixing of streams due to the random placement of the particles (which is not taken into account in the model) contributes to the destruction of the boundary layers.

No matter what the mixing mechanism, an empirical Reynolds number dependence may be incorporated into an analog of equation (5). In this manner, the asymptotic Sherwood numbers were combined as

$$\frac{1}{Sh_B} = \left\{ \left[\left(\frac{1}{Sh_B^{(1)}} \right)^n + \left(\frac{1}{Sh_B^{(2)} + Sh_B^{(3)}} \right)^n \right] e^{-n\sigma Re_B} + \left(\frac{1}{Sh_B^{(4)}} \right)^n \right\}^{1/n} \quad (6)$$

The exponential term involving the Reynolds number will cause the contribution of the length-dependent term to become negligible compared to the length-independent term as the Reynolds number increases. There are now two parameters to fit to the data, n and σ . The values of these parameters are again dependent upon the geometric parameters of the tube.

The high Péclet number data were fitted excellently by the straight-tube model but less well by the sinusoidal PCT. For all values of the PCT geometrical parameters reported in the earlier publications, the

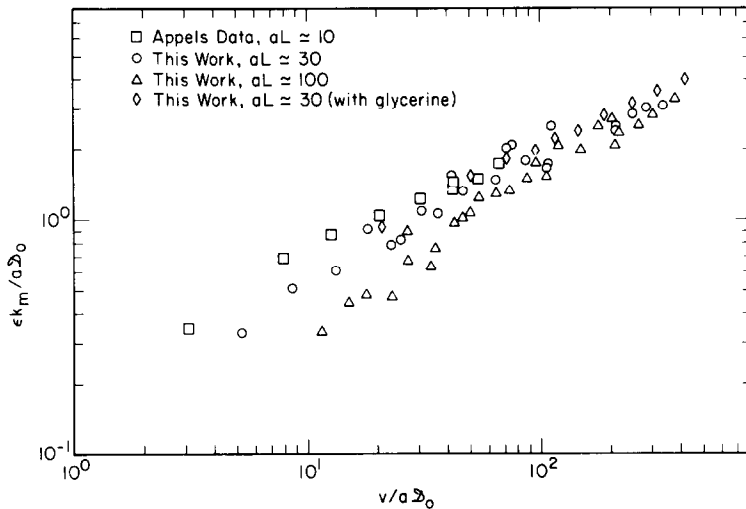


FIG. 3. Mass transfer limited Sherwood numbers for packed beds collected in this work. Appel's [15] data are also included.

PCT calculations consistently underestimate the mass transfer coefficient. The level of success obtained in fitting high Péclet number, mass transfer coefficients with the straight tube model was further emphasized when the data of other investigators were considered. However, neither model can satisfactorily fit the lower Péclet number data. Both models overestimate the Sherwood number in this region and, as with equation (5), a length dependence is not predicted. These lower Péclet number data point to a weakness in the model which will be discussed shortly.

The straight-tube calculations fit the collected data at higher Péclet numbers much better than the PCT calculations. On this basis, one can conclude that the PCT model is not successful in fitting packed bed mass transfer data. The higher level of complexity required

in calculating the PCT velocity profiles and asymptotic Sherwood numbers in a PCT geometry is not required. The PCT model was thought *a priori* to have been a better model for the bed because it would, in a sense, reproduce the constrictions and expansions that the actual fluid path must follow in a bed. This assumption has been proved wrong by this work. In the remainder of this work, the straight-tube model calculations are exploited.

THE EFFECT OF FLOW MALDISTRIBUTION IN A PACKED BED ON THE MASS TRANSFER COEFFICIENT

The low Péclet number, mass transfer coefficients obtained in this work show a stronger length dependence than is predicted by any model calculations.

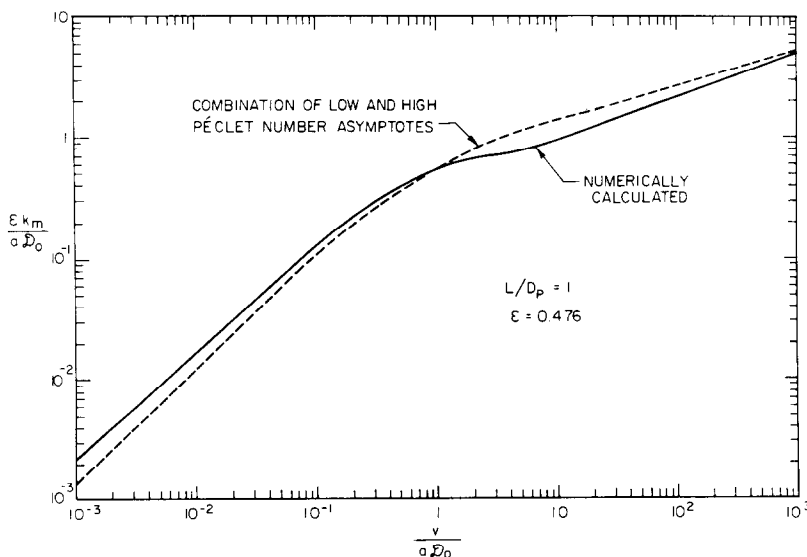


FIG. 4. Comparison of Sørensen and Stewart's [14] numerically calculated Sherwood numbers with those given by combining the asymptotes according to equation (5) with $n = 1$.

Table 2. Calculated results of [14] for the mass transfer coefficient in a simple cubic packed bed of uniformly sized spheres

$\frac{v}{aD_0}$	(1)	(2)	(3)	(4)	(5)
aL	4.9	9.9	15	∞	$(2)/(4)$
9.55	0.916	0.769	0.714	0.595	1.29
31.8	1.37	1.09	0.954	0.598	1.82
95.5	2.11	1.59	1.38	0.603	2.64
318	3.18	2.55	2.18	0.614	4.15

The full solution to the convective-diffusion equation will give a length-dependent coefficient for all values of the Péclet number, but this dependence is weakest in the lower Péclet number regions. Table 2 supports this statement. This table shows the numerically calculated k_m coefficients of [14] for a simple cubic packed bed of uniform size spheres. The 5th column gives the ratio of the k_m for a bed with $aL = 9.9$ to that for a deep bed ($aL = \infty$). For a Péclet number of 9.6, this ratio is 1.29, whereas the data collected in this work give a value for this ratio of 2.8 when the aL ratio is 10:100.

The larger-than-anticipated length effect can be explained by the presence of a non-uniform flow distribution in the bed. The effect of channeling on processes taking place in a bed has long been recognized in the literature. The fluid may find preferential paths of least resistance through the bed. These lower resistance paths may be near the wall where the local porosity is higher than the bulk average, but these paths are not necessarily confined to the wall. Dullien [18] has pointed out that in randomly packed beds there is a finite probability for flow connections of a larger than average size to form a network transversing the entire length of the bed.

Schlünder [19] has discussed the effect of flow maldistribution in an array of tubes. His array consisted of one large diameter tube embedded in a matrix of smaller sized tubes. Martin [20] has expanded upon this idea and applied it to a packed bed. In this work he considered the bed to consist of two regions, an annular outer region where the porosity is high and a central core region with the bulk porosity. Both workers have demonstrated that the overall mass transfer coefficient one would calculate by appropriately summing the contributions of each flow segment is lower than that of a composite system where the non-uniformities are neglected by an averaging process. Both workers have used the inappropriate limiting form of the mass transfer coefficient in their segmented flow channels. Schlünder [19] recommended for each model tube, the combination of the Graetz and Léveque solution, which is much like the combination suggested in equation (5). This combination cannot reproduce the correct linear dependence of k_m upon the Péclet number in the low Péclet number limit. Martin [20] has followed a similar procedure by applying the Ranz equation in

each segment, which predicts that the Sherwood number (defined on the particle diameter basis) reduces to 2 as the Péclet number approaches zero.

In the following analysis this idea of flow maldistribution is expanded upon, and in the process the correct limiting form for the Sherwood number is used.

The bed is now considered to be an array of two different size radii straight tubes. In this manner, the channeling flow is not conceptually limited to the confining wall region. Each of these tubes has its associated radius r_1 and r_2 , and its associated pore space ε_1 and ε_2 such that the total bed porosity is $\varepsilon_1 + \varepsilon_2$. Two dimensionless geometry parameters are generated by this model, the ratio of tube radii $r_2/r_1 = \delta$ and the porosity ratio $\varepsilon_2/\varepsilon_1$.

Since the pressure gradient is assumed to be identical in all tubes, the ratio of the flowrates can be calculated by using the Hagen-Poiseuille solution

$$q_2/q_1 = \delta^4. \quad (7)$$

The lower case q_i is used to designate the flowrate in a single tube of radius r_i . The upper case Q_i will be used to designate the flowrate in the entire collection of tubes of radius r_i .

The flowrate through the bed and the concentration at the exit of the bed may be written as

$$Q = Q_1 + Q_2 \quad (8)$$

$$Qc_L = Q_1c_{L,1} + Q_2c_{L,2}. \quad (9)$$

Let γ be the ratio of Q_2 to Q_1 ; equation (9) becomes

$$\frac{c_L}{c_F} = \frac{1}{1 + \gamma} \frac{c_{L,1}}{c_F} + \frac{\gamma}{1 + \gamma} \frac{c_{L,2}}{c_F}. \quad (10)$$

The overall Sherwood number for the bed is defined as usual:

$$\frac{c_L}{c_F} = \exp \left[- \frac{Sh_B aL}{Pe_B \varepsilon} \right]. \quad (11)$$

Equation (10) can now be rearranged to calculate the overall bed Sherwood number in terms of the Sherwood number in each individual tube matrix.

$$\frac{Sh_m}{aD_0} = \frac{\varepsilon}{\varepsilon_1} \frac{a_1 L Pe_B}{aL Pe_1} Sh_1 - \frac{\varepsilon}{aL Pe_1} Pe_B \ln \left\{ \frac{1}{1 + \gamma} + \frac{\gamma}{\gamma + 1} \right. \\ \times \exp \left[\frac{a_1 L Sh_1}{\varepsilon Pe_1} \left(1 - \frac{\varepsilon_1}{\varepsilon_2} \frac{a_2 L Pe_1}{a_1 L Pe_2} \frac{Sh_2}{Sh_1} \right) \right] \left. \right\}. \quad (12)$$

The Sherwood numbers Sh_i have been defined as

$$Sh_i = \frac{\varepsilon_i k_{m,i}}{a_i D_0} \quad (13)$$

and the Péclet numbers Pe_i as

$$Pe_i = \frac{v_i}{a_i D_0} \quad (14)$$

with v_i being the superficial velocity in the bed of tube size r_i only. With v_i so defined, the superficial velocity for the entire bed follows as $v_1 + v_2$.

Equation (12) can be placed into a more useful form by eliminating the tube variables on the right side in terms of the macroscopic parameters for the entire bed. It is straightforward to derive the following relationships

$$Pe_1 = \frac{1 + \varepsilon_2/\varepsilon_1 \delta}{1 + \varepsilon_2 \delta^2/\varepsilon_1} Pe_B \quad (15)$$

$$Pe_2 = \frac{1 + \varepsilon_1 \delta/\varepsilon_2}{1 + \varepsilon_1/\varepsilon_2 \delta^2} Pe_B \quad (16)$$

$$a_1 L = \frac{aL}{1 + \varepsilon_2/\varepsilon_1 \delta} \quad (17)$$

$$a_2 L = \frac{aL}{1 + \varepsilon_1 \delta/\varepsilon_2}. \quad (18)$$

These relationships can be used in equation (12) to write

$$Sh_B = Sh_1 - \frac{\varepsilon}{aL} Pe_B \ln \left\{ \frac{1}{1 + \varepsilon_2 \delta^2/\varepsilon_1} + \frac{\varepsilon_2 \delta^2/\varepsilon_1}{1 + \varepsilon_2 \delta^2/\varepsilon_1} \times \exp \left[h \frac{aL}{\varepsilon} \frac{Sh_1}{Pe_B} \left(1 - \frac{Sh_2}{\delta^4 Sh_1} \right) \right] \right\} \quad (19)$$

where h is defined as

$$h = h(\delta, \varepsilon_2/\varepsilon_1) = \frac{(1 + \varepsilon_2/\varepsilon_1)(1 + \varepsilon_2 \delta^2/\varepsilon_1)}{(1 + \varepsilon_2/\varepsilon_1 \delta)^2}. \quad (20)$$

By modeling the bed as an array of dual sized tubes, equation (19) can be used to calculate the overall conversion in the bed taking into account the flow distribution and the availability of reactive surface area in the network. The mass transfer coefficients for each size tube matrix must be known in order to make use of this result. Our attention is now turned to this matter.

The experimental data indicate that there is no significant length dependence for k_m in the higher Péclet number region. This suggests that the Sherwood numbers for each tube size matrix be empirically combined from asymptotic values as

$$\frac{1}{Sh_i} = \left\{ \left[\frac{1}{Sh_i^{(1)}} \right]^n + \left[\frac{1}{Sh_i^{(4)}} \right]^n \right\}^{1/n}. \quad (21)$$

These Sherwood numbers for the straight-tube model are

$$Sh_i^{(1)} = 1.20 Pe_i \quad (22)$$

$$Sh_i^{(4)} = 0.896 \left\{ \frac{\varepsilon}{[6(1-\varepsilon)]^{2/3}} \frac{1 + \varepsilon_j/\varepsilon_i \delta}{1 + \varepsilon_j/\varepsilon_i} \right\}^{1/3} Pe_i^{1/3}. \quad (23)$$

There are now three parameters to fit to the data, δ , $\varepsilon_2/\varepsilon_1$ and n .

Figure 5 is a plot of equation (19) compared with the data. The parameter values were determined as before in a least squares sense and were found to be $\delta = 1.56$, $\varepsilon_2/\varepsilon_1 = 0.0148$ and $n = 0.642$. Figure 6 illustrates this equation with the same fitted parameter set in comparison to the mass transfer data of other workers.

The channeling model fits the data collected in this work for all Péclet numbers. The root mean square deviation between the data and predicted Sherwood numbers is 10.8%. It also gives an excellent fit to the higher Péclet number data of the other workers. The low Péclet number data fit is not as good but is satisfactory.

The parameter set which fits the data collected in this work should not be expected to be the best set for other workers' beds. It is representative of the range, however, in which the values are expected to lie, and as seen in Fig. 6 does give a satisfactory correlation.

Great care was taken in packing the bed used in this study to generate a reproducible packing and to minimize large voids. This is reflected in the porosity value for the larger tube size. The larger void occupies only 1.46% of the total void volume of the bed in this study ($\varepsilon_2/\varepsilon$). A non-tamped, randomly dumped bed would be expected to give a larger porosity value for the bigger tubes. This would also be true for beds of non-uniform size particles. Both of the above-mentioned beds would exhibit larger channeling flows and hence lower apparent mass transfer coefficients. As a general rule, for a given Péclet number, the larger the fraction of fluid which channels through the bed, the smaller the apparent mass transfer coefficient.

In terms of the two-tube-size model, the effect of channeling becomes insignificant at large Péclet numbers. Most of the reactant passes through the bed unreacted in this situation, therefore the width of the flow channel has very little effect. At low Péclet numbers, however, the channeling effect will always be apparent since the conversion at low Péclet numbers is controlled dominantly by the larger channels. The larger tubes are 56% larger in diameter than the smaller tubes in this study and occupy only a small percentage of the void volume; yet they are the controlling resistance for conversion at the lower Péclet numbers.

SUMMARY

Equations (19) and (21) are the significant result of this work. The parameter values $\varepsilon = 0.4$, $n = 0.642$, $\varepsilon_2 = 0.00584$, and $\delta = 1.56$ may be used in these equations to correlate the transport-controlled mass transfer coefficient in packed beds at low Reynolds numbers (< 1).

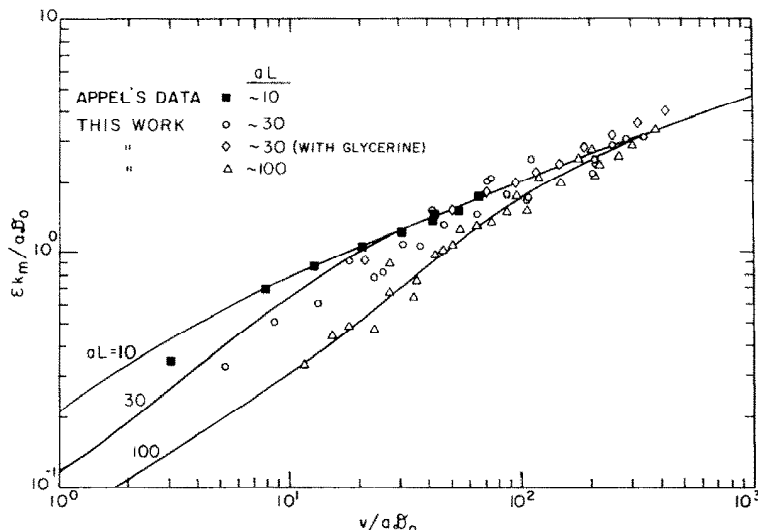


FIG. 5. Combination of straight-tube asymptotic Sherwood numbers incorporating a channeling effect according to equation (19) with $c = 0.4$, $n = 0.642$, $\epsilon_2 = 0.00584$ and $\delta = 1.56$.

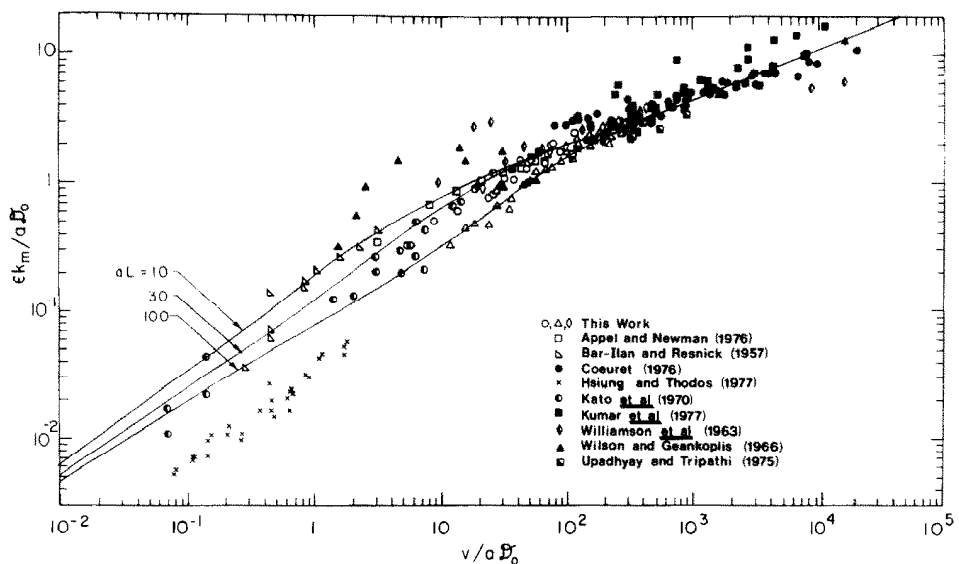


FIG. 6. Comparison of straight-tube channeling model with literature data.

The complexity of the periodically constricted tube model was shown not to be required to model the mass transfer characteristics of a packed bed. Rather, at low Reynolds numbers a straight-tube model which incorporates a channeling flow effect was shown to represent the data adequately.

REFERENCES

1. J. Newman and W. Tiedemann, Flow-through porous electrodes. In *Advances in Electrochemistry and Electrochemical Engineering*, Vol. 11. John Wiley, New York (1978).
2. P. Fedkiw and J. Newman, Mass transfer at high Péclet numbers, *AIChE J.* **23**, 255 (1977).
3. P. Fedkiw and J. Newman, Low Péclet number behavior of the transfer rate in packed beds, *Chem. Engr Sci.* **33**, 1043 (1978).
4. P. Fedkiw and J. Newman, Numerical calculations for the asymptotic, diffusion dominated mass transfer coefficient in packed bed reactors, *Chem. Engr Sci.* **33**, 1563 (1978).
5. P. Fedkiw and J. Newman, Entrance region (Léveque-like) mass transfer coefficients in packed bed reactors, *AIChE J.* **25**, 1077 (1979).

Acknowledgement—This work was supported by the Assistant Secretary of Conservation and Renewable Energy, Office of Advanced Conservation Technology, Electrochemical Systems Research Division of the U.S. Department of Energy under Contract Number W-7405-ENG-48.

6. P. W. Appel and J. Newman, Application of the limiting-current method to mass transfer in packed beds at very low Reynolds numbers, *AIChE J* **22**, 979 (1976).
7. M. Bar-Ilan and W. Resnick, Gas phase mass transfer in fixed beds at low Reynolds numbers, *Ind. Engr. Chem.* **49**, 313 (1957).
8. T. H. Hsiung and G. Thodos, Mass transfer factors from actual driving forces for the flow of gases through packed beds, *Int. J. Heat Mass Transfer* **20**, 331 (1977).
9. K. Kato, H. Kubota and C. Y. Wen, Mass transfer in fixed and fluidized beds, *Chem. Engng Prog. Symp. Ser.* **66** (No. 105), 87 (1970).
10. S. Kumar, S. N. Upadhyay and V. K. Mathur, Low Reynolds number mass transfer in packed beds of cylindrical particles, *Ind. Engng Chem. Process Des. Dev.* **16**, 1 (1977).
11. J. Williamson, K. E. Bazaire and C. J. Geankoplis, Liquid phase mass transfer at low Reynolds numbers, *Ind. Engr Chem. Fund.* **2**, 126 (1963).
12. E. J. Wilson and C. J. Geankoplis, Liquid mass transfer at very low Reynolds numbers in packed beds, *Ind. Engr Chem. Fund.* **5**, 9 (1966).
13. S. N. Upadhyay and G. Tripathi, Liquid phase mass transfer in fixed and fluidized beds of large particles, *J. Chem. Engr Data* **20**, 20 (1975).
14. J. P. Sørensen and W. E. Stewart, Computation of slow flow through ducts and packed beds—III heat and mass transfer in a simple cubic array of spheres, *Chem. Engr Sci.* **29**, 827 (1974).
15. P. Fedkiw, Mass transfer controlled reactions in packed beds at low Reynolds numbers, Ph.D. dissertation, University of California, Berkeley (1979).
16. S. W. Churchill and R. Usagi, A general expression for the correlation of rates of transfer and other phenomena, *AIChE J* **8**, 1121 (1972).
17. A. Acrivos, On the solution of the convection equation in laminar boundary layer flows, *Chem. Engr Sci.* **17**, 457 (1962).
18. F. A. L. Dullien, Single phase flow through porous media and pore structure, *Chem. Engr J.* **10**, 1 (1975).
19. E. U. Schlünder, On the mechanism of mass transfer in heterogeneous systems—in particular in fixed beds, fluidized beds and in bubble trays, *Chem. Engr Sci.* **32**, 845 (1977).
20. H. Martin, Low Péclet number particle-to-fluid heat and mass transfer in packed beds, *Chem. Engr Sci.* **33**, 913 (1978).
21. F. Coeuret, L'électrode poreuse percolante (EPP)—I. Transfert de matière en lit fixe, *Electrochim. Acta* **21**, 185 (1976).

COEFFICIENTS DE TRANSFERT MASSIQUE DANS DES LITS FIXES A DES NOMBRES DE REYNOLDS TRES PETITS

Résumé—Des coefficients de transfert massique ont été mesurés avec précision dans des lits fixes par la technique électrochimique aux faibles nombres de Reynolds ($0,00271 < v/av < 0,198$). Aux petits nombres de Péclet, les mesures montrent une forte dépendance vis-à-vis de la longueur du lit, mais cette dépendance diminue aux débits les plus élevés. Les résultats sont représentés par un modèle simple du volume des pores du lit.

Le lit se comporte comme si 1,46% du volume de pore était dans les pores dont le diamètre est 56% plus grand que le diamètre des pores restant. Les plus grands pores causent une mauvaise distribution de l'écoulement et ils réduisent nettement le transfert massique aux plus faibles nombres de Péclet.

STOFFTRANSPORTKoeffizienten IN FESTBETTEN BEI SEHR KLEINEN REYNOLDS-ZAHLEN

Zusammenfassung—Genaue, transportbestimmte Stoffübergangskoeffizienten für Festbetten wurden mit einem elektrochemischen Verfahren für kleine Reynolds-Zahlen gemessen ($0,00271 < v/av < 0,198$). Bei kleinen Péclet-Zahlen zeigen die Werte einen starken Einfluß der Länge des Bettes, aber dieser Einfluß verringert sich bei höheren Durchsätzen. Die Ergebnisse wurden mit Hilfe eines geraden Zwei-Größen-Porenmodells für das Porenvolumen des Bettes korrielt. Das Bett verhielt sich so, als ob 1,46% des Porenvolumens aus Poren bestände, deren Durchmesser 56% größer als der Durchmesser der verbleibenden Poren war. Die größeren Poren haben eine Verschlechterung der Strömungsverteilung zur Folge und verringern deutlich den Stoffübergang bei kleinen Péclet-Zahlen.

КОЭФФИЦИЕНТЫ МАССОПЕРЕНОСА В ПЛОТНЫХ СЛОЯХ ПРИ ОЧЕНЬ НИЗКИХ ЗНАЧЕНИЯХ ЧИСЛА РЕЙНОЛЬДСА

Аннотация — Электрохимическим методом получены точные значения коэффициентов массо-переноса плотных слоев при малых значениях числа Рейнольдса ($0,00271 < v/av < 0,198$). В случае малых значений числа Пекле наблюдается сильная зависимость значений коэффициентов от длины слоя, однако эта зависимость уменьшается с увеличением скорости течения. Результаты для пористого объема слоя обобщаются с помощью двухмерной модели прямых пор.

Слой ведет себя, как если бы 1,46% пористого объема находилось в порах, диаметр которых на 56% превышает диаметр остальных пор. Поры большего размера вызывают нарушения в распределении потока и значительно снижают перенос массы при более малых значениях числа Пекле.